Mineralogical Magazine (2023), **87**, 528–533
doi:10.1180/mgm.2023.14

CAMBRIDGE UNIVERSITY PRESS

Article

Zincorietveldite, $Zn(UO_2)(SO_4)_2(H_2O)_5$, the zinc analogue of rietveldite from the Blue Lizard mine, San Juan County, Utah, USA

Anthony R. Kampf[1], Travis A. Olds[2], Jakub Plášil[3] and Joe Marty[1]

[1]Mineral Sciences Department, Natural History Museum of Los Angeles County, 900 Exposition Boulevard, Los Angeles, CA, USA; [2]Section of Minerals and Earth Sciences, Carnegie Museum of Natural History, 4400 Forbes Avenue, Pittsburgh, PA, USA and [3]Institute of Physics of the CAS, Na Slovance 1999/2, 18200 Prague 8, Czech Republic

Abstract

The new mineral zincorietveldite (IMA2022-070), $Zn(UO_2)(SO_4)_2(H_2O)_5$, was found in the Blue Lizard mine, San Juan County, Utah, USA, where it occurs as yellow to orange–yellow blades in a secondary assemblage with bobcookite, coquimbite, halotrichite, libbyite, metavoltine, rhomboclase, römerite, tamarugite and voltaite. The streak is very pale yellow. Crystals are transparent with vitreous lustre. The tenacity is brittle, the Mohs hardness is ~2½ and the fracture is curved. Cleavage is excellent on {010}, good on {100} and fair on {001}. The mineral is easily soluble in H_2O and has a calculated density of 3.376 g·cm^{-3}. The mineral is optically biaxial (+) with $\alpha = 1.568(2)$, $\beta = 1.577(2)$ and $\gamma = 1.595(2)$; $2V = 70(1)°$. Electron microprobe analyses provided $(Zn_{0.720}Mg_{0.109}Fe_{0.091}Mn_{0.046}Co_{0.035})_{\Sigma 1.00}(UO_2)(SO_4)_2(H_2O)_5$. Zincorietveldite is orthorhombic, $Pmn2_1$, $a = 12.8712(9)$, $b = 8.3148(4)$, $c = 11.2959(4)$ Å, $V = 1208.90(11)$ Å^3 and $Z = 4$. Zincorietveldite is the Zn analogue of rietveldite. The structural unit is a uranyl-sulfate chain that is also found in the structures of bobcookite, oldsite, oppenheimerite and svornostite.

Keywords: zincorietveldite, rietveldite, new mineral, uranyl sulfate, crystal structure, Raman spectroscopy, Blue Lizard mine, Red Canyon, Utah, USA

(Received 23 January 2023; accepted 19 February 2023; Accepted Manuscript published online: 3 March 2023; Associate Editor: Daniel Atencio)

Introduction

Uranyl-sulfate minerals are widespread phases found in nearly all sandstone-hosted uranium–vanadium deposits in the southwestern United States, and worldwide. In Red Canyon, Utah, sulfates dominate the secondary uranyl mineralisation occurring on mine walls; in fact, many of the deposits in this region were first located by prospectors who noticed bright yellow and green encrustations on the uranium-bearing layers exposed at the surface. In the decades since mining ceased in Red Canyon, the remaining exposed (and unexposed) ore has undergone numerous periods of dissolution, crystallisation, and fluctuations in humidity and pH, which have led to an explosion in the diversity of uranyl species found underground.

Zincorietveldite, the new mineral described herein, is the 25th new mineral to be first described from the Blue Lizard mine in southeast Utah, USA, all within the last 10 years (see, for instance, Plášil *et al.*, 2023; Kampf *et al.*, 2023a). Zincorietveldite is named as the zinc analogue of rietveldite with Zn dominant in each of the two octahedrally coordinated cation sites. The new mineral and name (symbol Zrvd) were approved by the Commission on New Minerals, Nomenclature and Classification of the International Mineralogical Association (IMA2022-070, Kampf *et al.*, 2023b). The description is based on five cotype specimens, all micromounts, deposited in the collections of the Natural History Museum of Los Angeles County, 900 Exposition Boulevard, Los Angeles, CA 90007, USA, catalogue numbers 76262, 76264, 76265, 76266 and 76267. Specimen 76267 is also a cotype for libbyite (Kampf *et al.*, 2023c).

Occurrence

Zincorietveldite was found by two of the authors (ARK and JM) in efflorescent crusts on mine walls underground in the Blue Lizard mine (37°33'26"N, 110°17'44"W), Red Canyon, White Canyon District, San Juan County, Utah, USA. The mine is ~72 km west of the town of Blanding, Utah, and ~22 km southeast of Good Hope Bay on Lake Powell. Detailed historical and geological information on the Blue Lizard mine is described elsewhere (e.g. Kampf *et al.*, 2015a), and is primarily derived from a report by Chenoweth (1993). Abundant secondary uranium mineralisation in Red Canyon is associated with post-mining oxidation of asphaltite-rich sandstone beds laced with uraninite and sulfides in the damp underground environment. Zincorietveldite is a relatively rare mineral found in association with bobcookite, coquimbite, halotrichite, libbyite, metavoltine, rhomboclase, römerite, tamarugite, voltaite and other potentially new minerals on matrix comprised mostly of subhedral to euhedral, equant quartz crystals that are recrystallised counterparts of the original grains of the sandstone.

We have also confirmed the occurrence of zincorietveldite at the Widowmaker mine, on Fry Mesa, also in the White Canyon district; however, our description of the species is based solely

Corresponding author: Anthony R. Kampf; Email: akampf@nhm.org
Cite this article: Kampf A.R., Olds T.A., Plášil J. and Marty J. (2023) Zincorietveldite, $Zn(UO_2)(SO_4)_2(H_2O)_5$, the zinc analogue of rietveldite from the Blue Lizard mine, San Juan County, Utah, USA. *Mineralogical Magazine* **87**, 528–533. https://doi.org/10.1180/mgm.2023.14

© The Author(s), 2023. Published by Cambridge University Press on behalf of The Mineralogical Society of the United Kingdom and Ireland.

https://doi.org/10.1180/mgm.2023.14 Published online by Cambridge University Press

on material from the Blue Lizard mine. The Widowmaker mine should not be considered a cotype locality.

Morphology, physical properties and optical properties

Zincorietveldite occurs as subparallel groups of yellow to orange–yellow blades up to ~1 mm in length (Fig. 1). Blades are elongate on [001], flattened on {010} and exhibit the forms {100}, {010}, {110}, {011}, {01$\bar{1}$}, {101}, {$\bar{1}$0$\bar{1}$}, {111} and {11$\bar{1}$} (Fig. 2). No twinning was observed, but merohedral twinning is likely because of the noncentrosymmetric space group. The streak is very pale yellow and the mineral is nonfluorescent. Crystals are transparent with a vitreous lustre. The tenacity is brittle and the fracture is curved. The Mohs hardness is ~2½ based on scratch tests. There are three cleavages: excellent on {010}, good on {100} and fair on {001}. Crystals sink very slowly in pure methylene iodide (3.32 g·cm^{-3}). The mineral is soluble in Clerici solution, so the density could not be measured. The calculated density based upon the empirical formula is 3.376 g·cm^{-3}. The mineral is easily soluble in room-temperature H_2O. Zincorietveldite is optically biaxial (+) with $\alpha = 1.568(2)$, $\beta = 1.577(2)$ and $\gamma = 1.595(2)$ measured in white light. The 2V measured directly on a spindle stage is 70(1)°; the calculated 2V is 71.2°. Dispersion is strong, $r > v$. The optical orientation is $X = \mathbf{b}$, $Y = \mathbf{a}$ and $Z = \mathbf{c}$. The mineral is pleochroic with X = yellow, Y = colourless and Z = light yellow; $Y < Z < X$. The Gladstone–Dale compatibility (Mandarino, 2007) $1 - (K_p/K_c)$ is –0.002 (superior) based on the empirical formula using $k(UO_3) = 0.118$, as provided by Mandarino (1976).

Raman spectroscopy

Raman spectroscopy was done on a Horiba XploRA PLUS micro-Raman spectrometer using an incident wavelength of 532 nm, laser slit of 100 μm, 1800 gr/mm diffraction grating and a 100× (0.9 NA) objective. The spectrum, recorded from 4000 to 60 cm^{-1}, is shown in Fig. 3.

The spectrum of zincorietveldite is very similar to that of rietveldite and the band assignments indicated in Fig. 3 are the same as those previously proposed for rietveldite (Kampf *et al.*, 2017). Using the empirically derived equation of Libowitzky (1999), the sharp band at 3540 cm^{-1} is consistent with hydrogen bond O···O distances of ~2.96 Å. This value matches well with our proposed hydrogen bonding scheme for which 14 of the 18 O···O distances are in the range 2.92 to 3.00 Å (see Table 4). According to the empirical relationship of Bartlett and Cooney (1989), the ν_1 UO_2^{2+} band at 860 cm^{-1} corresponds to a U–O_{Ur} bond length of ~1.75 Å, in excellent agreement with U–O_{Ur} bond lengths from the X-ray data: 1.750(6) and 1.766(6) Å.

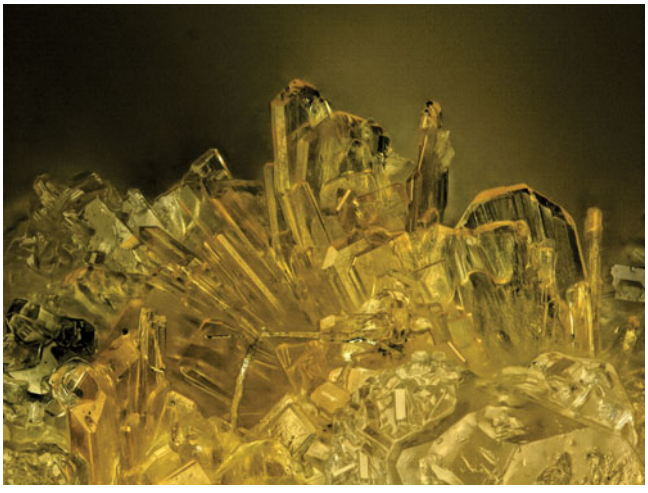

Figure 1. Zincorietveldite blades on cotype specimen #76263. The field of view is 1.12 mm across.

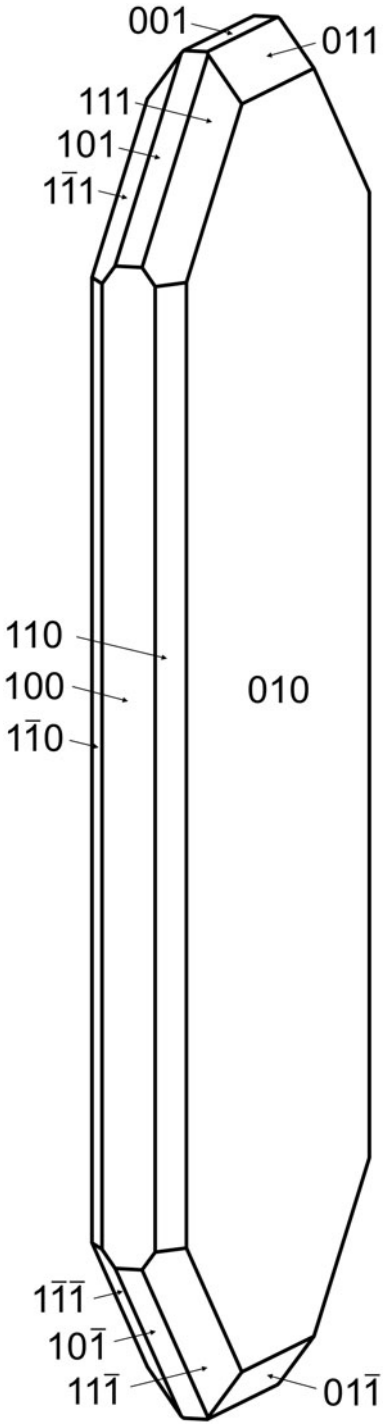

Figure 2. Crystal drawing of zincorietveldite; clinographic projection.

https://doi.org/10.1180/mgm.2023.14 Published online by Cambridge University Press

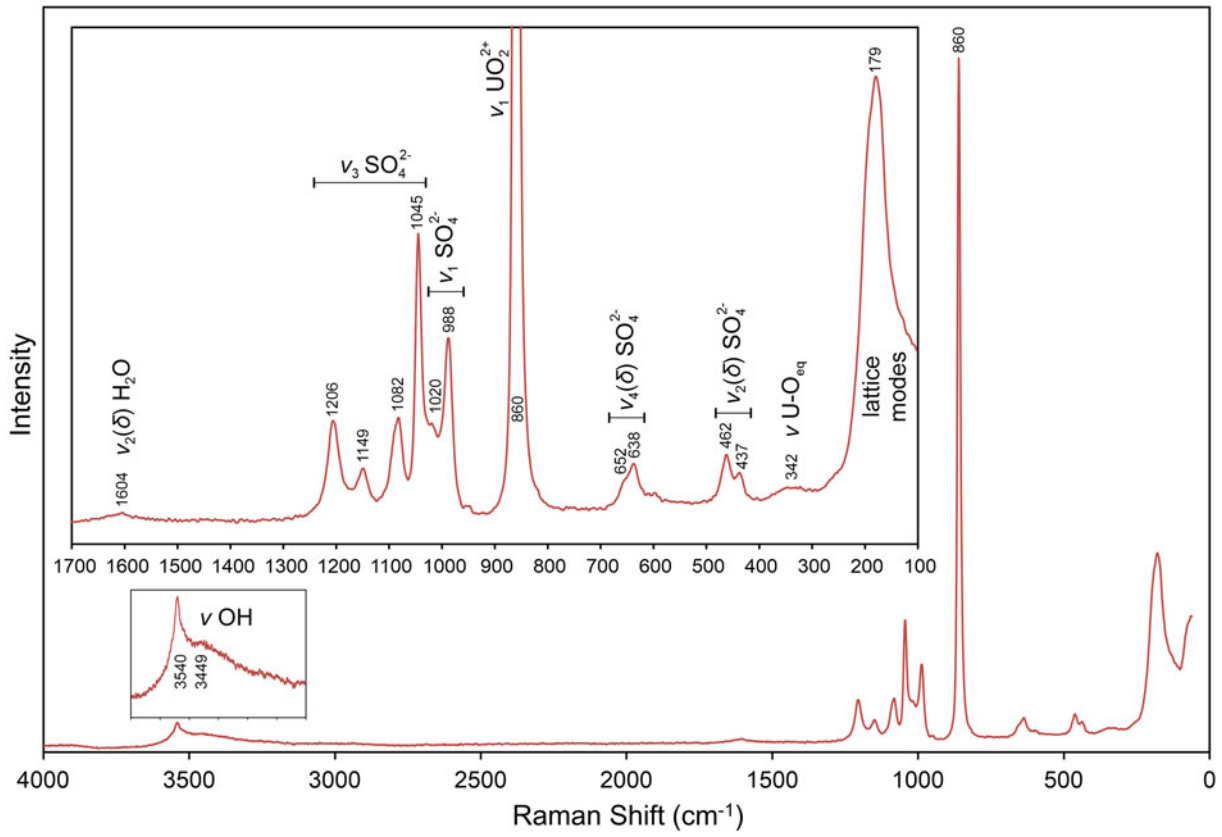

Figure 3. Raman spectrum of zincorietveldite recorded using a 532 nm diode laser.

Chemical composition

Electron probe microanalyses (6 points) were done using a JEOL JXA-8230 electron microprobe operating in wavelength dispersive spectroscopy mode using *Probe for EPMA* software (https://www.probesoftware.com). Analytical conditions were 15 kV accelerating voltage, 1 nA beam current and a beam diameter of 10 μm. Because insufficient material is available for a direct determination of H_2O, it has been calculated based upon the structure determination (S = 2 and O = 15 atoms per formula unit). The analytical results are given in Table 1.

The empirical formula (based on 15 O apfu) is $(Zn_{0.675}Mg_{0.102}Fe_{0.085}Mn_{0.043}Co_{0.033})_{\Sigma 0.938}(U_{1.028}O_2)(SO_4)_2(H_{1.991}O)_5$. Adjusting for full occupancy of the Zn and U sites, the empirical

Table 1. Analytical data (in wt.%) for zincorietveldite.

Constituent	Mean	Range	S.D.	Probe standard
MgO	0.68	0.65–0.70	0.033	MgO
MnO	0.50	0.37–0.62	0.104	spessartine
FeO	1.01	0.65–1.28	0.231	hematite
CoO	0.41	0.27–0.55	0.114	Co metal
ZnO	9.10	8.28–9.59	0.526	ZnS
SO_3	26.53	24.78–28.14	1.148	anhydrite
UO_3	48.73	46.26–50.26	1.394	UO_2
H_2O*	14.86			
Total	101.82			

* Based on structure
S.D. – standard deviation

Table 2. Data collection and structure refinement details for zincorietveldite.

Crystal data	
Structural formula	$(Zn_{0.88}Mg_{0.12})_{\Sigma 1.00}US_2O_{15}$
Space group	$Pmn2_1$ (#31)
Unit cell dimensions (Å)	a = 12.8712(9)
	b = 8.3148(4)
	c = 11.2959(4)
V (Å^3)	1208.90(11)
Z	4
Density (for above formula) (g·cm^{-3})	3.365
Absorption coefficient (mm^{-1})	15.553
Data collection	
Diffractometer	Rigaku R-Axis Rapid II
X-ray radiation/power	Mo$K\alpha$ (λ = 0.71075 Å)/50 kV, 40 mA
Temperature (K)	293(2)
F(000)	1127
Crystal size (μm)	190 × 80 × 20
θ range (°)	3.04 to 27.48
Index ranges	$-14 \le h \le 16$, $-10 \le k \le 10$, $-12 \le l \le 14$
Reflections collected/unique	6954/2485; R_{int} = 0.035
Reflections with $I > 2\sigma I$	2174
Completeness to θ = 27.48°	99.7%
Refinement	
Refinement method	Full-matrix least-squares on F^2
Parameter/restraints	189/1
GoF	1.074
Final R indices [$I > 2\sigma I$]	R_1 = 0.0308, wR_2 = 0.0683
R indices (all data)	R_1 = 0.0361, wR_2 = 0.0716
Absolute structure parameter	0.000(9)
Largest diff. peak/hole ($e-$ Å^{-3})	+4.45/–0.99

$R_{int} = \Sigma|F_o^2 - F_o^2(\text{mean})|/\Sigma[F_o^2]$. GoF = $S = \{\Sigma[w(F_o^2 - F_c^2)^2]/(n-p)\}^{½}$. $R_1 = \Sigma||F_o| - |F_c||/\Sigma|F_o|$. $wR_2 = \{\Sigma[w(F_o^2 - F_c^2)^2]/\Sigma[w(F_o^2)^2]\}^{½}$; $w = 1/[\sigma^2(F_o^2) + (aP)^2 + bP]$ where a is 0.0325, b is 0.5911 and P is $[2F_c^2 + \text{Max}(F_o^2, 0)]/3$.

https://doi.org/10.1180/mgm.2023.14 Published online by Cambridge University Press

Table 3. Atom coordinates and displacement parameters (Å^2) for zincorietveldite.

	x/a	*y/b*	*z/c*	U_{eq}	U^{11}	U^{22}	U^{33}	U^{23}	U^{13}	U^{12}
Zn1*	0	0.6777(3)	0.28060(17)	0.0263(8)	0.0134(10)	0.0395(16)	0.0260(13)	0.0072(9)	0	0
Zn2*	½	0.6643(2)	0.24863(16)	0.0204(7)	0.0155(10)	0.0253(13)	0.0204(11)	0.0011(8)	0	0
U	0.24791(2)	0.88701(3)	0.93401(15)	0.01318(13)	0.01588(19)	0.01445(19)	0.00921(19)	0.0009(3)	−0.00065(17)	−0.00114(11
S1	0.2737(2)	0.7625(4)	0.6263(3)	0.0178(6)	0.0223(10)	0.0214(15)	0.0097(13)	0.0008(11)	0.0003(14)	0.0011(11)
S2	0.24643(15)	0.7436(4)	0.2456(3)	0.0139(6)	0.0161(12)	0.0144(15)	0.0112(15)	0.0006(11)	0.0008(9)	−0.0007(8)
O1	0.1607(5)	0.7507(11)	0.6238(8)	0.0343(18)	0.019(3)	0.051(5)	0.033(4)	−0.001(4)	0.000(4)	−0.011(3)
O2	0.3250(7)	0.6194(8)	0.5794(8)	0.036(2)	0.048(5)	0.020(5)	0.041(5)	−0.009(4)	0.001(4)	0.012(3)
O3	0.3103(6)	0.9011(8)	0.5553(7)	0.0317(19)	0.037(5)	0.022(5)	0.037(5)	0.014(3)	0.001(4)	0.005(3)
O4	0.3133(5)	0.7867(9)	0.7503(5)	0.0279(18)	0.030(4)	0.047(5)	0.007(3)	−0.002(3)	−0.010(3)	−0.004(3)
O5	0.3376(6)	0.6417(9)	0.2524(8)	0.031(2)	0.020(4)	0.022(4)	0.052(6)	0.008(4)	−0.001(4)	0.002(3)
O6	0.2674(7)	0.8970(12)	0.3040(12)	0.041(3)	0.048(6)	0.040(7)	0.034(7)	−0.016(4)	−0.004(5)	−0.004(4)
O7	0.1602(6)	0.6624(11)	0.3040(7)	0.033(2)	0.020(4)	0.050(5)	0.028(5)	0.019(4)	0.006(4)	−0.001(3)
O8	0.2171(6)	0.7758(9)	0.1221(7)	0.0296(16)	0.043(3)	0.032(5)	0.015(3)	0.005(3)	0.003(4)	−0.002(4)
O9	0.1184(5)	0.8428(9)	0.8997(6)	0.0234(15)	0.021(3)	0.034(4)	0.015(3)	−0.009(3)	0.001(3)	−0.004(3)
O10	0.3786(5)	0.9331(8)	0.9678(6)	0.0269(17)	0.025(3)	0.025(4)	0.031(4)	−0.010(3)	0.001(3)	−0.007(3)
OW1	0.2884(7)	0.5950(8)	0.9473(9)	0.0350(19)	0.061(5)	0.019(4)	0.025(5)	0.003(3)	0.012(6)	−0.001(3)
OW2	0	0.6385(19)	0.0970(16)	0.056(5)	0.038(8)	0.085(12)	0.044(10)	−0.002(8)	0	0
OW3	0	0.7112(15)	0.4649(9)	0.035(3)	0.021(5)	0.066(9)	0.018(7)	−0.015(5)	0	0
OW4	0	0.9259(17)	0.2402(16)	0.060(5)	0.041(7)	0.030(8)	0.108(14)	−0.003(8)	0	0
OW5	0	0.4130(19)	0.2895(16)	0.044(4)	0.027(6)	0.059(9)	0.045(9)	−0.012(8)	0	0
OW6	½	0.6355(16)	0.0670(13)	0.036(4)	0.042(8)	0.044(8)	0.024(7)	0.009(5)	0	0
OW7	0	0.5845(16)	0.7677(14)	0.036(4)	0.032(7)	0.026(7)	0.051(10)	−0.007(6)	0	0
OW8	½	0.7151(15)	0.4277(14)	0.047(3)	0.034(5)	0.087(10)	0.019(6)	−0.013(8)	0	0
OW9	½	0.9138(13)	0.2119(12)	0.033(3)	0.032(6)	0.024(6)	0.041(8)	−0.004(5)	0	0

* Refined occupancies: Zn1 = $Zn_{0.875(14)}Mg_{0.125(14)}$; Zn2 = $Zn_{0.856(13)}Mg_{0.144(13)}$

Table 4. Selected bond distances (Å) for zincorietveldite.

Zn1–O7 (×2)	2.083(7)	U–O9	1.750(6)	S1–O1	1.458(6)	Hydrogen bonds	
Zn1–OW2	2.099(18)	U–O10	1.766(6)	S1–O2	1.461(7)	OW1···O2	2.745(12)
Zn1–OW3	2.101(10)	U–O6	2.328(10)	S1–O3	1.481(8)	OW1···O7	2.764(12)
Zn1–OW4	2.114(14)	U–O8	2.351(8)	S1–O4	1.504(7)	OW2···O9 (×2)	3.190(17)
Zn1–OW5	2.204(16)	U–O3	2.354(7)	<S1–O>	1.459	OW3···O1 (×2)	2.758(10)
<Zn1–O>	2.114	U–O4	2.390(7)			OW4···O10 (×2)	3.229(16)
		U–OW1	2.488(7)	S2–O5	1.450(8)	OW5···O4 (×2)	2.954(12)
Zn2–OW6	2.065(15)	<U–O_{Ur}>	1.758	S2–O7	1.457(8)	OW6···O10 (×2)	3.134(13)
Zn2–OW8	2.067(15)	<U–O_{eq}>	2.382	S2–O6	1.461(10)	OW7···O1 (×2)	2.971(13)
Zn2–OW7	2.079(14)			S2–O8	1.469(9)	OW8···O2 (×2)	2.940(13)
Zn2–O5 (×2)	2.099(8)			<S2–O>	1.476	OW9···O10 (×2)	3.174(14)
Zn2–OW9	2.116(11)						
<Zn2–O>	2.088						

formula is $(Zn_{0.720}Mg_{0.109}Fe_{0.091}Mn_{0.046}Co_{0.035})_{\Sigma 1.00}(UO_2)(SO_4)_2(H_2O)_5$. The simplified formula is $(Zn,Mg,Fe,Mn,Co)(UO_2)(SO_4)_2(H_2O)_5$. The ideal formula is $Zn(UO_2)(SO_4)_2(H_2O)_5$, which requires ZnO 13.18, UO_3 46.31, SO_3 25.93, H_2O 14.58, total 100 wt.%.

X-ray crystallography

Powder X-ray diffraction (PXRD) data were recorded using a Rigaku R-Axis Rapid II curved imaging plate microdiffractometer with monochromatised Mo*K*α radiation. A Gandolfi-like motion on the φ and ω axes was used to randomise the sample. Observed *d* values and intensities were derived by profile fitting using *JADE Pro* software (Materials Data, Inc.). The powder data are presented in Supplementary Table S1 (see below). The unit-cell parameters refined from the powder data using *JADE Pro* with whole pattern fitting are *a* = 12.871(3), *b* = 8.343(2), *c* = 11.314(2) Å and *V* = 1214.9(4) Å^3.

The single-crystal structure data were collected at room temperature using the same diffractometer and radiation noted above. The Rigaku *CrystalClear* software package was used for processing the structure data, including the application of an empirical absorption correction using the multi-scan method with *ABSCOR* (Higashi, 2001). The structure was solved using the intrinsic-phasing algorithm of *SHELXT* (Sheldrick, 2015a). *SHELXL-2016* (Sheldrick, 2015b) was used for the refinement of the structure. The structure solution located all non-hydrogen atoms, which were refined with anisotropic displacement parameters. The Zn1 and Zn2 sites were refined with joint occupancies by Zn and Mg yielding $Zn_{0.875}Mg_{0.125(14)}$ and $Zn_{0.856}Mg_{0.144(13)}$, respectively. These correspond to site scattering values of 55.500 and 54.816, respectively, for a total site scattering of 110.316. For comparison, the total site-scattering value corresponding to full site occupancies with the cation ratios indicated by the electron probe microanalyses is 109.476. The H atoms locations could not be found in the difference-Fourier maps. The two largest electron density residuals, 4.44 and 3.55 e^-, located 0.89 and 0.87 Å from the U site, respectively, are presumed to be ripple effects. Data collection and refinement details are given in Table 2,

https://doi.org/10.1180/mgm.2023.14 Published online by Cambridge University Press

Table 5. Bond valence analysis for zincorietveldite. Values are expressed in valence units.*

	Zn1	Zn2	U	S1	S2	Hydrogen bonds		Σ
						Accepted	Donated	
O1				1.55		0.20, 0.14		1.89
O2				1.54		0.21, 0.14		1.89
O3			0.52	1.47				1.99
O4			0.48	1.39		0.14		2.01
O5		$0.34^{\times 2\downarrow}$			1.59			1.92
O6			0.55		1.54			2.09
O7	$0.35^{\times 2\downarrow}$				1.56	0.20		2.11
O8			0.52		1.51			2.03
O9			1.87			0.10		1.97
O10			1.81			0.10, 0.10, 0.11		2.12
OW1			0.39				−0.21, −0.20	−0.02
OW2	0.34						$-0.10^{\times 2\rightarrow}$	0.14
OW3	0.34						$-0.20^{\times 2\rightarrow}$	−0.06
OW4	0.33						$-0.10^{\times 2\rightarrow}$	0.13
OW5	0.26						$-0.14^{\times 2\rightarrow}$	−0.02
OW6		0.37					$-0.11^{\times 2\rightarrow}$	0.15
OW7		0.36					$-0.14^{\times 2\rightarrow}$	0.08
OW8		0.37					$-0.14^{\times 2\rightarrow}$	0.09
OW9		0.32					$-0.10^{\times 2\rightarrow}$	0.12
Σ	1.97	2.10	6.14	5.95	6.20			

U^{+6}–O and S^{+6}–O bond-valence parameters from Gagné and Hawthorne (2015). Hydrogen-bond strengths based on O–O bond lengths from Ferraris and Ivaldi (1988). Negative values indicate donated hydrogen-bond contributions.

atom coordinates and displacement parameters in Table 3, selected bond distances in Table 4 and a bond-valence analysis in Table 5. The crystallographic information file has been deposited with the Principal Editor of *Mineralogical Magazine* and is available as Supplementary material (see below).

Description of the structure

Zincorietveldite is isostructural with rietveldite. The U site in the structure is surrounded by seven O atoms forming a squat UO_7 pentagonal bipyramid. This is the most typical coordination for U^{6+}, particularly in uranyl sulfates, where the two short apical bonds of the bipyramid constitute the uranyl group. Four of the five equatorial O atoms of the UO_7 bipyramid participate in SO_4 tetrahedra; the other is an H_2O group. The linkages of pentagonal bipyramids and tetrahedra form an infinite $[(UO_2)(SO_4)_2(H_2O)]^{2-}$ chain along [001] (Fig. 4). The chains are linked in the [100] direction by $Zn1O_2(H_2O)_4$ and $Zn2O_2(H_2O)_4$ octahedra, which share O vertices with SO_4 tetrahedra in the chains (Fig. 5). A heteropolyhedral sheet parallel to {010} is thereby formed. Adjacent sheets are linked only by hydrogen bonding (Fig. 4).

The $[(UO_2)(SO_4)_2(H_2O)]^{2-}$ chain in the structures of rietveldite and zincorietveldite is also found in the structures of bobcookite, $Na(H_2O)_2Al(H_2O)_6[(UO_2)_2(SO_4)_4(H_2O)_2]\cdot 8H_2O$ (Kampf *et al.* 2015a), oldsite, $K_2Fe[(UO_2)(SO_4)_2]_2\cdot 8H_2O$ (Plášil *et al.*, 2023), oppenheimerite, $Na_2(H_2O)_2[(UO_2)(SO_4)_2(H_2O)]$ (Kampf *et al.* 2015b), svornostite, $K_2Mg[(UO_2)(SO_4)_2]_2\cdot 8H_2O$ (Plášil *et al.*, 2015), synthetic $K_2[(UO_2)(SO_4)_2(H_2O)](H_2O)$ (Ling *et al.*, 2010) and synthetic $Mn(UO_2)(SO_4)_2(H_2O)_5$ (Tabachenko *et al.*, 1979). The chains in bobcookite and oppenheimerite are geometrical isomers of the chain in the structures of oldsite, rietveldite and zincorietveldite.

Studies of the synthetic phases of general formula $M(UO_2)(SO_4)_2(H_2O)_5$, in which M = Mg, Mn, Fe, Co, Ni, Cu, Zn or Cd (Kornyakov *et al.*, 2021; Serezhkin and Serezhkina, 1978; Soares Rocha, 1960; Tabachenko *et al.*, 1979), show that these phases occur in two polytypes (Table 6). Rietveldite and zincorietveldite

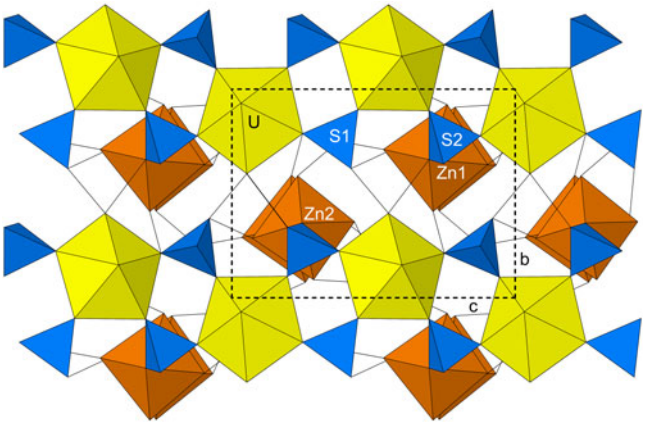

Figure 4. The structure of zincorietveldite viewed down [100]. Hydrogen bonds are shown as black lines. The unit-cell outline is shown by dashed lines.

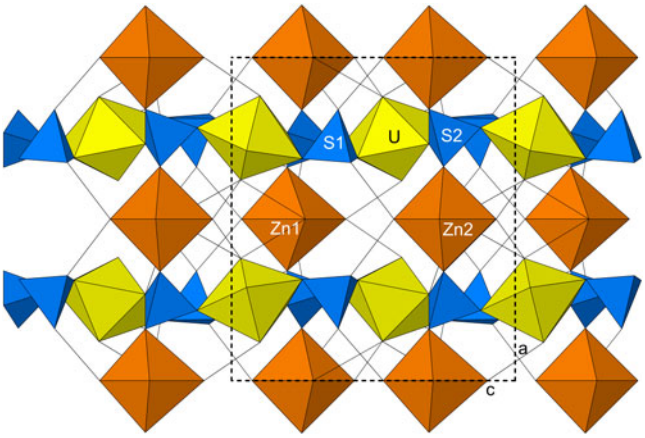

Figure 5. The structure of zincorietveldite viewed down [010]. Hydrogen bonds are shown as black lines. The unit-cell outline is shown by dashed lines

https://doi.org/10.1180/mgm.2023.14 Published online by Cambridge University Press

Table 6. Comparison of related minerals and synthetic phases.

Phase	Polytype	Space group	*a* (Å)	*b* (Å)	*c* (Å)	β (°)	Reference
Zincorietveldite	2*O*	$Pmn2_1$	12.871	8.315	11.296		This work
Rietveldite	2*O*	$Pmn2_1$	12.958	8.318	11.297		Kampf *et al.* (2017)
$Zn(UO_2)(SO_4)_2(H_2O)_5$	2*O*	$Pmn2_1$	12.869	8.282	11.292		Kornyakov *et al.* (2021)
$Fe(UO_2)(SO_4)_2(H_2O)_5$	2*O*	$Pmn2_1$	12.958	11.28	8.297		Kornyakov *et al.* (2021)
$Fe(UO_2)(SO_4)_2(H_2O)_5$	1*M*	$P2_1$	6.489	11.28	8.297	90.78	Serezhkin and Serezhkina (1978)
$Mg(UO_2)(SO_4)_2(H_2O)_5$	1*M*	$P2_1$	6.388	11.304	8.231	90.345	Kornyakov *et al.* (2021)
$Co(UO_2)(SO_4)_2(H_2O)_5$	2*O*	$Pmn2_1$	12.920	8.299	11.296		Kornyakov *et al.* (2021)
$Mn(UO_2)(SO_4)_2(H_2O)_5$	1*M*	$P2_1$	6.511	11.383	8.344	90.773	Kornyakov *et al.* (2021)

are isostructural with the synthetic phases with space group $Pmn2_1$ and have double the *a* cell parameter of the phases with space group $P2_1$.

Acknowledgements. Structures Editor Peter Leverett and an anonymous reviewer are thanked for their constructive comments on the manuscript. We are grateful to retired miner Dan Shumway of Blanding, Utah, for advice and assistance in our collecting efforts in Red Canyon. This study was funded, in part, by the John Jago Trelawney Endowment to the Mineral Sciences Department of the Natural History Museum of Los Angeles County. JP acknowledges the support of the Czech Science Foundation (GACR 20-11949S).

Supplementary material. The supplementary material for this article can be found at https://doi.org/10.1180/mgm.2023.14.

Competing interests. The authors declare none.

References

Bartlett J.R. and Cooney R.P. (1989) On the determination of uranium-oxygen bond lengths in dioxouranium(VI) compounds by Raman spectroscopy. *Journal of Molecular Structure*, **193**, 295–300.

Chenoweth W.L. (1993) The geology and production history of the uranium deposits in the White Canyon Mining District, San Juan County, Utah. *Utah Geological Survey Miscellaneous Publication*, 93–3.

Ferraris G. and Ivaldi G. (1988) Bond valence vs. bond length in O···O hydrogen bonds. *Acta Crystallographica*, **B44**, 341–344.

Gagné O.C. and Hawthorne F.C (2015) Comprehensive derivation of bond-valence parameters for ion pairs involving oxygen. *Acta Crystallographica*, **B71**, 562–578.

Higashi T. (2001) *ABSCOR. Rigaku Corporation*, Tokyo.

Kampf A.R., Plášil J., Kasatkin A.V. and Marty J. (2015a) Bobcookite, NaAl$(UO_2)_2(SO_4)_4 \cdot 18H_2O$, and wetherillite, $Na_2Mg(UO_2)_2(SO_4)_4 \cdot 18H_2O$, two new uranyl sulfate minerals from the Blue Lizard mine, San Juan County, Utah, USA. *Mineralogical Magazine*, **79**, 695–714.

Kampf A.R., Plášil J., Kasatkin A.V., Marty J. and Čejka J. (2015b) Fermiite, $Na_4(UO_2)(SO_4)_3 \cdot 3H_2O$, and oppenheimerite, $Na_2(UO_2)(SO_4)_2 \cdot 3H_2O$, two new uranyl sulfate minerals from the Blue Lizard mine, San Juan County, Utah, USA. *Mineralogical Magazine*, **79**, 1123–1142.

Kampf A.R., Sejkora J., Witzke T., Plášil J., Čejka J., Nash B.P. and Marty J. (2017) Rietveldite, $Fe(UO_2)(SO_4)_2(H_2O)_5$, a new uranyl sulfate mineral from Giveaway-Simplot mine (Utah, USA), Willi Agatz mine (Saxony, Germany) and Jáchymov (Czech Republic). *Journal of Geosciences*, **62**, 107–120.

Kampf A.R., Plášil J., Olds T.A., Ma C. and Marty J. (2023a) Shinarumpite, a new cobalt uranyl sulfate mineral from the Scenic mine, San Juan County, Utah, USA, structurally related to leydetite. *Mineralogical Magazine*, **87**, https://doi.org/10.1180/mgm.2022.128.

Kampf, A.R., Olds, T.A., Plášil, J. and Marty, J. (2023b) Zincorietveldite, IMA 2022-070. CNMNC Newsletter 70, *Mineralogical Magazine*, **87**, https://doi.org/10.1180/mgm.2022.135

Kampf A.R., Olds T.A., Plášil J., Nash B. and Marty J. (2023c) Libbyite, $(NH_4)_2(Na_2\square)[(UO_2)_2(SO_4)3(H_2O)]_2 \cdot 7H_2O$, a new mineral with uranyl-sulfate sheets from the Blue Lizard mine, San Juan County, Utah, USA. *Mineralogical Magazine*, **87**, https://doi.org/10.1180/mgm.2023.26

Kornyakov I.V., Tyumentseva O.S., Krivovichev S.V., Tananaev I.G. and Gurzhiy V.V. (2021) Crystal chemistry of the $M^{2+}[(UO_2)(T^{6+}O_4)_2(H_2O)](H_2O)_4$ (M^{2+} = Mg, Mn, Fe, Co, Ni and Zn; T^{6+} = S, Se) compounds: the interplay between chemical composition, pH and structural architecture. *CrystEngComm*, **23**, 1140–1148.

Libowitzky E. (1999) Correlation of O–H stretching frequencies and O–H···O hydrogen bond lengths in minerals. *Monatshefte für Chemie*, **130**, 1047–1059.

Ling J., Sigmon G.E., Ward M., Roback N. and Burns P.C. (2010) Syntheses, structures, and IR spectroscopic characterization of new uranyl sulfate/selenate 1D-chain, 2D-sheet and 3D framework. *Zeitschrift für Kristallographie*, **225**, 230–239.

Mandarino J.A. (1976) The Gladstone-Dale relationship – Part 1: derivation of new constants. *The Canadian Mineralogist*, **14**, 498–502.

Mandarino J.A. (2007) The Gladstone–Dale compatibility of minerals and its use in selecting mineral species for further study. *The Canadian Mineralogist*, **45**, 1307–1324.

Plášil J., Hloušek J., Kasatkin A.V., Novák M., Čejka J. and Lapčák L. (2015) Svornostite, $K_2Mg[(UO_2)(SO_4)_2]_2 \cdot 8H_2O$, a new uranyl sulfate mineral from Jáchymov, Czech Republic. *Journal of Geosciences*, **60**, 113–121.

Plášil J., Kampf A.R., Ma C. and Desor J. (2023) Oldsite, $K_2Fe^{2+}[(UO_2)(SO_4)_2]_2(H_2O)_8$, a new uranyl sulfate mineral from Utah, USA: its description and implications for the formation and occurrences of uranyl sulfate minerals. *Mineralogical Magazine*, **87**, 151–159, https://doi.org/10.1180/mgm.2022.106

Serezhkin V.N. and Serezhkina L.B. (1978) X-ray diffraction study of double uranyl sulphates $M(UO_2)(SO_4) \cdot 5H_2O$. *Russian Journal of Inorganic Chemistry*, **23**, 414–416.

Sheldrick G.M. (2015a) SHELXT – Integrated space-group and crystal-structure determination. *Acta Crystallographica*, **A71**, 3–8.

Sheldrick G.M. (2015b) Crystal Structure refinement with *SHELX*. *Acta Crystallographica*, **C71**, 3–8.

Soares Rocha N. (1960) Synthesis and X-Ray Data of Magnesium Uranyl Sulphate: $MgUO_2(SO_4)_2 \cdot nH_2O$. *Anais da Academia Brasileira de Ciências*, **32**, 341–343.

Tabachenko V.V., Serezhkin V.I., Serezhkina L.B. and Kovba L.M. (1979) Crystal structure of manganese sulfatouranylate $MnUO_2(SO_4)_2(H_2O)_5$. *Soviet Journal of Coordination Chemistry*, **5**, 1219–1223.